

## Dimers of aromatic molecules: (Benzene)<sub>2</sub>, (toluene)<sub>2</sub>, and benzene–toluene

K. Law, Mark Schauer, and E. R. Bernstein

Citation: *The Journal of Chemical Physics* **81**, 4871 (1984); doi: 10.1063/1.447514

View online: <http://dx.doi.org/10.1063/1.447514>

View Table of Contents: <http://aip.scitation.org/toc/jcp/81/11>

Published by the *American Institute of Physics*

---

---

**COMPLETELY  
REDESIGNED!**



**PHYSICS  
TODAY**

*Physics Today* Buyer's Guide  
Search with a purpose.

# Dimers of aromatic molecules: (Benzene)<sub>2</sub>, (toluene)<sub>2</sub>, and benzene–toluene<sup>a)</sup>

K. S. Law, Mark Schauer, and E. R. Bernstein

Department of Chemistry, Condensed Matter Sciences Laboratory, Colorado State University, Fort Collins, Colorado 80523

(Received 1 June 1984; accepted 26 July 1984)

The optical absorption spectra of the first excited singlet states of the benzene, toluene, and toluene–benzene dimers, created in a supersonic molecular jet, are reported. The absorption spectra are detected through two-color time of flight mass spectroscopy; this method eliminates fragmentation of dimers and higher clusters and the dimer spectra are uniquely observed. The benzene dimer observed in this experiment is suggested to have a parallel stacked and displaced configuration of  $C_{2h}$  symmetry. Both the toluene and toluene–benzene dimers have two configurations: parallel stacked and displaced [based on (benzene)<sub>2</sub>] and perpendicular. (Benzene)<sub>2</sub>, (toluene)<sub>2</sub>, and toluene–benzene form excimers in the excited state for the parallel stacked displaced configurations. The transformation of (benzene)<sub>2</sub> to the excimer takes place at the  $0^0$  with a  $\sim 0$  cm<sup>-1</sup> barrier while the excimer is formed for toluene–benzene with a  $\sim 900$  cm<sup>-1</sup> barrier. An exciton analysis of the (benzene)<sub>2</sub>  $0_0^0$  and  $6_0^1$  yields  $M_{12}$ , the excitation exchange interaction, equal to  $\sim 1.6$  cm<sup>-1</sup>.

## I. INTRODUCTION

One of the most important applications of molecular jet spectroscopy has been to the study of intermolecular interactions and dynamics. Studies of chromophore solute molecules surrounded by inert gases and simple alkanes have been suggested to be useful in the modeling of solution behavior.<sup>1</sup> In like manner, aromatic dimers, trimers, tetramers, etc. may be thought of as potential model systems for pure condensed phases. Even if the geometry and dynamics of either of these small cluster model systems are quite different from those of the condensed phases per se, the molecular jet generated clusters serve as an important component of our understanding and modeling of the collective properties of condensed matter.

Jet generated aromatic dimers have been studied by various techniques: (tetrazine)<sub>2</sub>,<sup>2</sup> (benzoic acid)<sub>2</sub>,<sup>3</sup> (benzene)<sub>2</sub>,<sup>4</sup> and (benzene–tetrazine)<sub>2</sub><sup>5</sup> have been examined by optical spectroscopy and molecule beam electric resonance (MBER) studies have been reported for (benzene)<sub>2</sub>,<sup>6,7</sup> (hexafluorobenzene)<sub>2</sub>,<sup>7</sup> and (benzene–hexafluorobenzene).<sup>7</sup> Photoionization time of flight mass spectroscopy (TOMFS) studies have thus far only been reported for (benzene)<sub>2</sub>.<sup>8,9</sup>

The above studies have two pertinent and common goals—the elucidation of dimer geometry and energy dynamics. The only well documented dimer structures are those of (tetrazine)<sub>2</sub> and (benzene–tetrazine) for which high resolution rotational structure has been reported and analyzed for the optical transitions. Specific and detailed intermolecular interactions seem to play an important role in determining the relative orientations of the two monomer subunits. The gas phase structure of the dimers does not

appear to be necessarily the same as expected from known crystal structures.<sup>2,3</sup> Nonetheless, Klemperer *et al.*,<sup>6,7</sup> using the MBER technique, have suggested that the relative orientations of the two subunits in (benzene)<sub>2</sub>, (hexafluorobenzene)<sub>2</sub>, and (hexafluorobenzene–benzene) are consistent with the nearest neighbor translationally inequivalent molecule orientations found in the crystal.<sup>10,11</sup> As in (benzene)<sub>2</sub>, the two monomer subunits in (hexafluorobenzene)<sub>2</sub> are stated to be arranged in a perpendicular fashion. In the (hexafluorobenzene–benzene) dimer the two molecules are arranged in a parallel stacked orientation. One must understand, however, that the MBER technique selects for polar molecules and clusters only and thus may not render unique results.

Numerous theoretical treatments of the relative orientations of benzene molecules in the benzene dimer have appeared.<sup>12</sup> No unanimous agreement exists among those studies. In general, four arrangements of the benzene molecules have been suggested: the perpendicular or “T”, the parallel stacked, the parallel side by side, and parallel displaced and tilted configurations.

Energy dynamics have also been explored in some dimer systems and are found to depend significantly on geometry. In (tetrazine)<sub>2</sub>, two distinct conformations have been characterized<sup>2</sup>: one dimer conformation is planar with two translationally equivalent molecules and the other dimer conformation is perpendicular with symmetry inequivalent rings giving rise to two electronic transitions. In (benzoic acid)<sub>2</sub>, electronic excitation is found largely localized in one or the other molecular subunit.<sup>3</sup> Shortening of the  $S_1$  lifetime in (benzene)<sub>2</sub> can be attributed to the rearrangement of a ground state configuration, assumed to be perpendicular, to an excimer configuration upon excitation.<sup>8</sup>

The work reported in this paper is an outgrowth of the studies of the toluene dimer. The data for the toluene system are quite complicated and somewhat perplexing. In order to understand these latter results, data have been collected on the toluene–benzene and benzene dimers in the hope that

<sup>a)</sup>Supported in part by grants from ONR and ARO-D.

these additional systems would serve as a guide for the (toluene)<sub>2</sub> species and prove a test for our techniques. Four experiments on toluene–benzene, (benzene)<sub>2</sub>, and (toluene)<sub>2</sub> were carried out: two-color photoionization time of flight mass spectroscopy (two-color MS), determination of  $S_1$  lifetimes, ionization energy dependence of the TOFMS intensity, and changes in these results with isotopic substitution.

Through these experiments, the toluene–benzene dimer is found to have two distinct conformations. We suggest that in one conformation the two molecules are parallel with their centers displaced from one another. We call this the parallel displaced configuration. The molecules in the parallel displaced configuration rearrange into an excimer conformation upon excitation to  $S_1$ ; the barrier for this geometry change, a shift in position and a shortening of the interring distance, is found to be  $\sim 900 \text{ cm}^{-1}$ . The other toluene–benzene dimer geometry features the two subunits in a perpendicular arrangement giving rise to more than one possible local configuration. The parallel displaced configuration is about ten times more prevalent for our molecular jet expansion conditions than the perpendicular geometries. The observation of two possible configurations for the toluene–benzene dimer has led to a more complete interpretation of the toluene dimer and to a reevaluation of the geometry of the benzene dimer.

An isotope effect study of the benzene dimers ( $h_6:h_6$ ,  $d_6:d_6$ ,  $h_6:k_6$ ) leads to the conclusion that excitation exchange or exciton effects dominate the  $0_0^0$  transition. We thereby conclude that the ground state conformation of this species is parallel displaced with  $C_{2h}$  symmetry. This parallel displaced conformation transforms, upon excitation, into an excimer geometry. The barrier height for this transformation is zero. The data are also consistent with the less likely geometry of two side-by-side molecules in a common plane (dimer symmetry  $D_{2h}$ ).

The absorption spectrum of the toluene dimer shows great complexity. Ionization energy dependence of the absorption features strongly suggest that two different geometries are present. These are most likely the parallel displaced and perpendicular configurations; unfortunately, both spectra fall in the same region.

## II. EXPERIMENTAL PROCEDURES

The supersonic molecular jet apparatus employed in this work and the procedures for obtaining the two-color MS data have been described in detail previously.<sup>1(a)</sup> Information specific to the present experiments only will be presented below.

Two Quanta-Ray Nd:YAG pumped dye laser systems provide the excitation and ionization laser beams. The initial excitation process to  $S_1$  is accomplished typically with Coumarin 500 in the dye laser; however, for  $d_6^*:d_6$  and  $d_6^*:h_6$  LDS 698 is used. The output of the Coumarin dye is doubled and the output of the LDS 698 must be doubled and mixed with  $1.06 \mu\text{m}$ . Ionization ( $S_1$  to  $I$ ) is affected by various frequency doubled dye outputs. Most of the detailed information about laser energy and intensity is included in the figure captions. The excitation and ionization beam widths are typically  $\sim 0.25 \text{ cm}^{-1}$ . However, in the experiment for

which infrared mixing is required (doubled LDS 698 +  $1.06 \mu\text{m}$ ), the excitation laser bandwidth is increased to  $\sim 1 \text{ cm}^{-1}$  ( $\sim \sqrt{0.25 + 0.85}$ ).

The  $S_1$  lifetimes of the dimeric species are determined by varying the time delay between the pump and the ionization laser pulses while monitoring the two-color MS signal intensity. The ion signals are processed through a Tektronix 7912AD programmable digitizer, with 7A16P and 7B90P plug-in units, which is interfaced to an HP 9845S computer. The programmable digitizer is delay triggered from an Evans digital delay board to minimize intensity fluctuations due to time jitter. The two laser pulses are monitored by the same 1P28 photomultiplier tube. In order to obtain an accurate measurement of the time delay between the two pulses, a small portion of the one-color MS signal due to the pump beam is intentionally monitored. This latter signal is usually too small to be observed, but in this case it is generated by increased pump laser intensity to serve as a calibration mark for zero time delay. Thus, the time delays between the two laser pulses can be accurately measured between the weak one-color MS and intense two-color MS signals. Each data point is an average of 640 laser shots. Laser power drifts are minimized by completing the particular lifetime experiment in a short period of time ( $\sim 1/2 \text{ h}$ ); observed power drifts in the lasers are roughly 5% per half hour. The lifetime data should be accurate to within  $\pm 5 \text{ ns}$ .

Three different nozzles are employed in this apparatus to obtain two-color MS spectra: a  $25 \mu\text{m}$  cw nozzle; a  $50 \mu\text{m}$  cw nozzle; and a  $0.5 \text{ mm}$  pulsed nozzle. The temperature of nozzle is kept at  $25^\circ\text{C}$  unless otherwise stated in the figure captions. No obvious differences in spectral features are observed as a function of nozzle types except for intensities. The  $0.5 \text{ mm}$  pulsed nozzle gives the most intense spectra. Lifetimes of the toluene dimer are found to depend on nozzle conditions, however.

Calibration for the absorption spectra is provided either by the optogalvanic effect for an Fe–Ne hollow cathode lamp or a calibrated McPherson  $1.0 \text{ m}$  monochromator. Absolute positions of spectral features are accurate to  $\pm 1.0 \text{ cm}^{-1}$  and relative positions are accurate to  $\pm 0.3 \text{ cm}^{-1}$  for sharp features.

Two additional experiments on the benzene dimer have been carried out: a Stark effect study performed by varying the potential between the plates of the mass spectrometer ( $300\text{--}2000 \text{ V}$  over a distance of  $\sim 1.0 \text{ cm}$ ); and a two photon absorption TOFMS detected study of the (benzene)<sub>2</sub>  $0_0^0$  transition.

## III. RESULTS

In this section the experimental data for each dimer will be reported separately for four experiments: two-color MS; ionization energy dependence of the absorption features;  $S_1$  lifetimes; and isotopic effects. Emission studies were not pursued for these systems because: (a) emission spectra of (benzene)<sub>2</sub> are well documented<sup>4</sup>; (b) the total emission of the toluene dimer is quite weak; and (c) significant intramolecular vibrational redistribution processes are expected for (toluene)<sub>2</sub> and toluene–benzene.<sup>13</sup>

TABLE I. Toluene-benzene ( $h_g^*$ :  $h_g$ ) transitions observed by two color-TOFMS detection between 37 230 and 38 200  $\text{cm}^{-1}$ .

Transition energy (vac $\text{cm}^{-1}$ )	Relative intensity	Dimer vibrational intervals ( $\text{cm}^{-1}$ )	$\Delta\nu^a$ ( $\text{cm}^{-1}$ )	Tentative assignments <sup>b</sup>	
$0_0^0$	37 230.5	100	0	-247.0	$0_0^0$ pd
	37 238.2	8	7.7	-235.1	$A_0^1$
	37 249.0	7	18.5	-225.3	$B_0^1$
	37 272.4	90	41.9	-201.4	$V_0^1$
	37 283.0	38	52.5	-191.6	$A_0^1 V_0^1$
	37 305.6	86	75.1	-170.9	$V_0^2$
	37 313.8	21	83.5	-162.9	$A_0^1 V_0^2$
	37 324.7	21	94.2	-152.3	$B_0^1 V_0^2$
	37 344.4	30	113.9	-132.7	
	37 375.0	17	144.9	-101.0	
	37 453.5	15		-24.2	$0_0^0$ p
	37 468.7	17		-8.8	
	37 470.6	19		-6.9	
	37 484.4	19		6.9	
	37 486.8	19		9.3	
	37 493.2	10		15.7	
	37 499.7	14		22.2	
	37 502.2	13		24.7	
	37 508.5	8		31	
	37 512.9	8		35.4	
	37 514.9	9		37.4	
$15_0^1$	37 563.5	7	0	-244.0	$15_0^1$ pd
	37 606.2	6	42.7	-201.3	$15_0^1 V_0^1$
	37 640.4	3	76.9	-167.1	$15_0^1 V_0^2$
$6a_0^1$	37 693.1	23	0	-243.4	$6a_0^1$ pd
	37 734.3	19	41.2	-202.2	$6a_0^1 V_0^1$
	37 768.9	18	75.8	-167.6	$6a_0^1 V_0^2$ ; $6b_0^1 A_0^1$
	37 926.5	5		-10.0	$6a_0^1$ p
	37 941.7	4		5.2	
	37 956.4	5		20.0	
$6b_0^1$	37 761.5	60	0	-246.0	$6b_0^1$ pd
	37 803.6	50	42.1	-204.0	$6b_0^1 V_0^1$
	37 816.1	20	54.6	-191.4	$6b_0^1 A_0^1 V_0^1$
	37 838.0	45	76.5	-169.5	$6b_0^1 V_0^2$
	37 846.2	12	84.7	-161.3	$6b_0^1 A_0^1 V_0^2$
	37 856.7	10	95.2	-150.8	$6b_0^1 B_0^1 V_0^2$
	37 876.9	15	115.4	-130.6	
	37 909.0	13	147.5	-98.5	
$1_0^1$	37 984.2	20	0	-245.8	$1_0^1$ pd; $6b_0^1$ p
	37 990.1	2	5.4	-240.4	$1_0^1 A_0^1$ pd
	38 000.1	5	15.4	-230.4	$1_0^1 B_0^1$ pd; $6b_0^1$ p
	38 015.1	4	30.4	-215.4	$6b_0^1$ p
	38 031.2	15	46.5	-199.3	$1_0^1 V_0^1$ pd; $6b_0^1$ p
	38 041.1	8	56.5	-189.4	$1_0^1 A_0^1 V_0^1$ pd
	38 064.6	14	79.9	-165.9	$1_0^1 V_0^2$ pd
$12_0^1$	38 160.1	20	0	-250.4	$12_0^1$ pd
$18a_0^1$	38 200.5	25	0	-242.0	$18a_0^1$ pd

<sup>a</sup> Shifts are relative to  $h_g^*$  transitions. For  $6a_0^1$  and  $1_0^1$  transitions shifts are relative to the more intense Fermi resonance components.

<sup>b</sup> Assignments are tentative. *A* and *B* refer to the bending modes, *V* indicates the stretching mode and pd and p indicate the absorption features are due to the parallel displaced and perpendicular conformations, respectively. No indication of pd or p implies an assignment to the geometry most recently stated.

## A. Toluene-benzene

### 1. Two-color MS

The  $0^0$  levels of toluene and benzene in their first excited states are separated by only  $608 \text{ cm}^{-1}$ . Thus, upon excitation

of the  $0^0$  and  $6^1$  levels of the benzene molecule in the mixed dimer, higher levels of the toluene molecule will also be accessed (i.e.,  $6a^1$ ,  $6b^1$ ,  $1^1$ ,  $12^1$ , and  $18a^1$ ). For notational convenience we will refer to the component of a dimer accessed by an asterisk:  $h_g^*:h_g$ ;  $h_g^*:d_g$ ;  $d_g^*:d_g$ ;  $h_g^*:h_g$ ; etc. ( $h_g$  and  $d_g$  represent toluene- $h_g$  and benzene- $d_g$ , respectively).

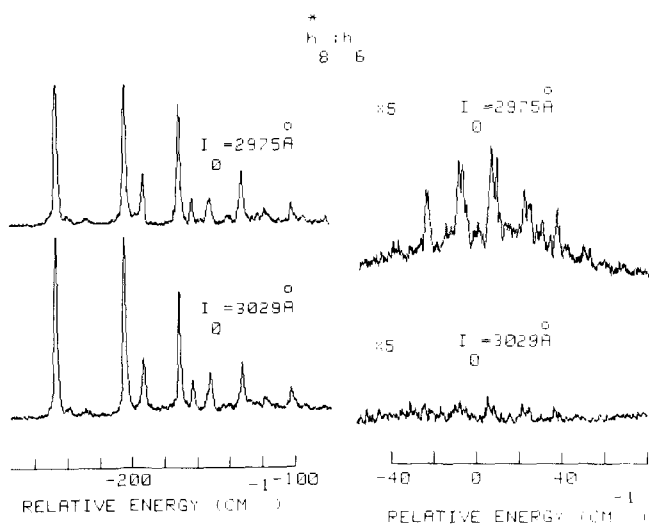


FIG. 1. Two-color TOF mass spectra of  $h_8^*:h_6$  near the toluene electronic origin. Energy scale is relative to  $h_8^*0_0^0$  at  $37\,477.5\text{ cm}^{-1}$ . Note the different ionization energy dependence of the absorption features. Experimental conditions:  $50\text{ }\mu\text{m}$  cw nozzle, nozzle temperature =  $25^\circ\text{C}$ , backing pressure =  $200\text{ psi}$ .

*a.*  $h_8^*:h_6:0_0^0$ . Figure 1 (top trace) describes the two-color MS spectrum of  $h_8^*:h_6$  near the toluene  $0_0^0$ . The spectrum in this region is free of congestion and without features of  $h_8^*:h_8$ . Two sets of peaks are obvious from the figures: one set is red shifted relative to the toluene  $0_0^0$  by  $250\text{--}100\text{ cm}^{-1}$  and the other set is in the proximity of the toluene  $0_0^0$  ( $-25\text{--}+35\text{ cm}^{-1}$ ). The more red shifted bands are roughly an order of magnitude more intense than the less red shifted ones. The positions of these features are tabulated in Table I.

The lower energy features can be analyzed as a stretching progression built on the  $-247\text{ cm}^{-1}$  feature. This latter band is thereby assigned as the  $0_0^0$  transition of one configuration of  $h_8^*:h_6$  (see Table I). The transitions near the toluene  $0_0^0$  bear no apparent relationship to the lower energy set. Moreover, they have a doublet structure and are not readily analyzed as a progression built on a given feature or a set of features (see Fig. 2). These weak transitions can be thought of

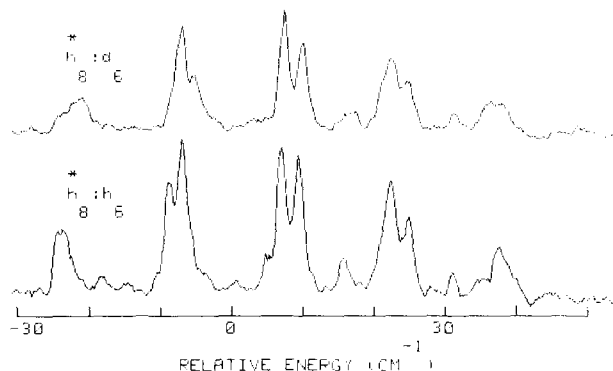


FIG. 2. Expanded traces of the two-color mass spectra of  $h_8^*:h_6$  and  $h_8^*:d_6$  near the  $h_8^*0_0^0$ . Energy scale is relative to the  $h_8^*0_0^0$ . Note that the spectral shifts due to isotopic substitution are minor ( $2\text{ cm}^{-1}$ ). Experimental conditions:  $0.5\text{ mm}$  pulsed nozzle, nozzle temperature =  $25^\circ\text{C}$ ; backing pressure =  $100\text{ psi}$ .

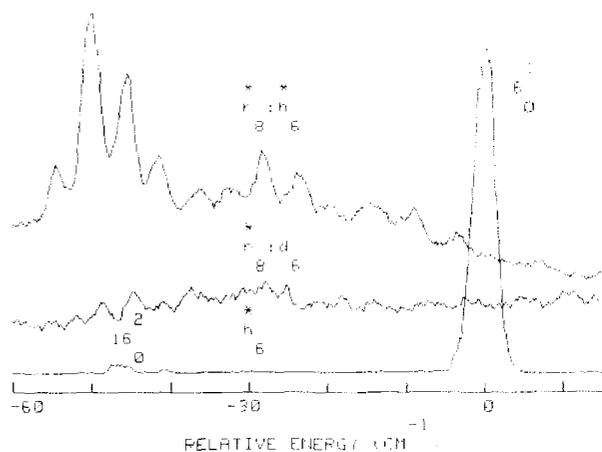


FIG. 3. Two-color mass spectra of  $h_8^*:h_6/h_8^*:h_8^*$  and  $h_8^*:d_6$  near the  $h_8^*6_0^1$ . Energy scale is relative to  $h_8^*6_0^1$  at  $38\,608.7\text{ cm}^{-1}$ . Absorption features of  $h_8^*:h_8$  can be identified by comparing these three spectra (see Table II). Experimental conditions (see Fig. 2).

as due to a number of similar configurations of  $h_8^*:h_6$ . Suggestions for geometries associated with these two sets of features will be considered in the Discussion section.

*b.*  $h_8^*:h_6:15_0^1;6a_0^1;6b_0^1$ , etc. The two-color MS spectrum of  $h_8^*:h_6$  remains relatively free of congestion up to the  $6b_0^1$  transition of toluene. The prominent absorption features in this spectral region are tabulated in Table I. Only the lower energy configuration is observed at  $15_0^1$  with two van der Waals stretching features. A similar spectrum is observed at  $6a_0^1$ . The higher energy configuration is apparently too weak to be observed. The absorption spectrum of  $h_8^*:h_6$  at  $6b_0^1$  is similar to that observed for the  $0_0^0$ . Bands due to both configurations are observed. It is not possible to assign all the features at  $1_0^1$ ,  $12_0^1$ , and  $18a_0^1$  uniquely because of overlap between transitions to different vibrations and different configurations (see Table I).

*c.*  $h_8^*:h_8:0_0^0$ . This spectral region exhibits complicated structure due to the overlap of  $6b_0^1$  ( $h_8^*:h_6$ ) and  $1_0^1$  ( $h_8^*:h_6$ ). By comparison with the  $d_8^*:h_8$  spectrum a feature specific to the  $h_8^*:h_8:0_0^0$  can be located at  $\sim -45\text{ cm}^{-1}$  from benzene- $h_6$  expected  $0_0^0$ .

*d.*  $h_8^*:h_8:6_0^1$ . Figure 3 presents the absorption spectrum of  $h_8^*:h_8$  and  $d_6: h_8^*$  near the  $6_0^1$  origin of  $h_6$ . Again, deuteration of the benzene moiety in the toluene benzene dimer aids in the identification of the  $h_8^*:h_8$  absorption bands. An intense doublet at  $-45\text{ cm}^{-1}$  from  $h_8^*6_0^1$  is clearly associated with  $h_8^*:h_8$ . The site splitting of the doublet is  $\sim 4.5\text{ cm}^{-1}$ . Table II summarizes these data.

## 2. Ionization energy dependence

The ionization potentials of toluene and benzene monomers are known.<sup>14</sup> In general, the ionization threshold for a cluster is a few hundred  $\text{cm}^{-1}$  lower in energy than the corresponding monomer threshold.<sup>15</sup> The onset of ionization is not sharp in most clusters. Two-color MS data have already been published for benzene clusters<sup>8</sup> and this same energy was employed for  $h_8^*:h_8$  and  $d_8^*:h_8$  ionization energy ( $\lambda_1 \sim 2789\text{ \AA}$ ). For  $h_8^*:h_6$  and  $d_8^*:h_6$  the toluene monomer ionization energy was used ( $\lambda_1 \sim 2975\text{ \AA}$ ). Using an ioniza-

TABLE II. The relative energies and the tentative assignments of the absorption features of  $h_6:h_8$  near the  $h_8^* 6_0^1$ .

Energy (vac $\text{cm}^{-1}$ )	Relative intensity	Dimer shifts ( $\text{cm}^{-1}$ )	Assignments <sup>b</sup>
38 555.9	31	-52.8	$h_8^*:h_6$
38 560.5	100	-48.2	$6_0^1 h_8^*; h_8 \text{pd}$
38 565.0	81	-43.7	$6_0^1 h_8^*:h_8 \text{pd}$
38 568.9	33	-39.8	$h_8^*:h_6$
38 574.1	27	-34.6	$h_8^*:h_6$
38 577.9	27	-30.8	$h_8^*:h_6$
38 582.2	33	-26.5	$h_8^*:h_8$
38 586.7	29	-22.0	$h_8^*:h_8$
38 590.5	23	-18.2	$h_8^*:h_8$
38 595.8	24	-12.9	$h_8^*:h_8$
38 600.9	22	-7.8	$h_8^*:h_8$
38 606.8	19	-1.9	$h_8^*:h_8$

<sup>a</sup> Dimer shifts are relative to  $h_8^* 6_0^1$ , 38 608.7  $\text{cm}^{-1}$ .

<sup>b</sup> Assignments are tentative and are derived from the comparison of the  $h_6:h_8^*/h_8^*:h_8$  and  $h_8^*:d_6$  spectra (see Fig. 3). pd = parallel displaced configuration.

tion beam wavelength of 2789 Å for  $h_8^*:h_6$  and  $d_8^*:h_6$ , no fragmentation was observed. This observation suggests that the binding energy of  $(h_8^*:h_6)^+$  is more than 2200  $\text{cm}^{-1}$ .

On the other hand, lowering the ionization beam energy by 600  $\text{cm}^{-1}$  (from  $\lambda_i = 2975$  to 3029 Å) causes a change in relative intensity of the  $h_8^*:h_6 0_0^0$  features at  $\sim -250 \text{ cm}^{-1}$  compared to those at  $-25 \text{ cm}^{-1}$ . The different ionization energy dependence of the two sets of absorption features suggests the existence of at least two distinct configurations for  $h_8^*:h_6$  (see Fig. 1). This trend is best seen for the  $0_0^0$  and  $6a_1^1$  transitions. Similar studies for  $h_8^*:h_8$  were inconclusive because of weak intensity and spectral congestion.

### 3. Lifetimes

The  $S_1$  lifetime for  $h_8^*:h_6$  is found to be  $\sim 40$  ns while the  $S_1$  lifetime of  $h_8^*$  is 103 ns.<sup>16</sup> This behavior has been previously explained to be due to excimer formation in  $h_8^*:h_6$ . By monitoring the  $S_1$  lifetime of both geometries of  $h_8^*:h_6$  and  $h_8^*:h_8$ , the excited state dynamics of this dimer can be ex-

TABLE III. The  $S_1$  lifetimes  $\tau$  of isotopically substituted toluene-benzene and benzene dimers at various vibronic levels.

Isotopic species	$S_1$ lifetime in ns <sup>a</sup>			
	$0_0^0$	$6b_1^1$	$12^1$	$6^1$
$h_8^*$	78			
$h_8^*$	103 <sup>b</sup>			
$h_8^*:h_6$	79	60	49	
⊥	75			
$h_8^*:h_8$				36
$h_8^*:h_6$	40			39
$h_8^*:d_6$	39			
$d_8^*:d_6$	46			
$d_8^*:h_6$	47			

<sup>a</sup>  $6b_1^1$ ,  $12^1$ —vibronic levels of toluene.  $6^1$ —vibronic level of benzene.

<sup>b</sup> See Ref. 16.

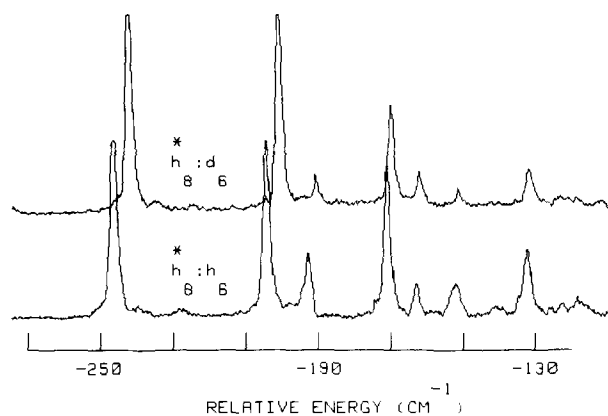


FIG. 4. Two-color mass spectra of  $h_8^*:d_6$  and  $h_8^*:h_6$  near the  $0_0^0$  of the parallel displaced configuration of  $h_8:h_6$ . Energy scale is relative to the  $h_8^* 0_0^0$  at 37 477.5. Note the unusual isotopic shifts (Table IV). Experimental conditions (see Fig. 2).

plored. The  $S_1$  lifetime study for the higher energy configuration was confined to the  $0_0^0$  because of congestion and low intensity for other vibronic levels. Note the  $S_1$  lifetimes of  $h_8^*:h_6$  are 75 ns at the  $0_0^0$ , 60 ns at the  $6b_1^1$ , and 49 ns at  $12^1$  (see Table III). The  $S_1$  lifetime of  $h_8^*:h_8$  at  $6^1$  (more than 1300  $\text{cm}^{-1}$  above the  $h_8^*:h_6 0_0^0$ ) is 36 ns. This latter lifetime is the same as the found for  $h_8^*:h_6$ . We suggest that this gradual decrease in the  $S_1$  lifetime of the lower energy dimer as higher vibronic states are probed is due to rearrangement of  $h_8^*:h_6$  and  $h_8^*:h_8$  into an excimer configuration. This transformation takes place with a finite barrier height.

### 4. Isotope effects

The effects of isotopic substitution on the toluene-benzene dimer has been examined at the  $0_0^0$  and  $6b_1^1$  transitions for both geometries. Both configurations have been studied at the  $0_0^0$ , but only the low energy one has been studied at the  $6b_1^1$ . The resulting spectra are presented in Figs. 2, 4, and 5. The relative shifts between the protonated and deuterated isotopic dimers ( $h_8^*:h_6$ ,  $h_8^*:d_6$ ,  $d_8^*:h_6$ ,  $d_8^*:d_6$ ) are listed in Table IV. The most striking features of these data are the unusual direction of the shifts and difference in shifts for the two configurations.

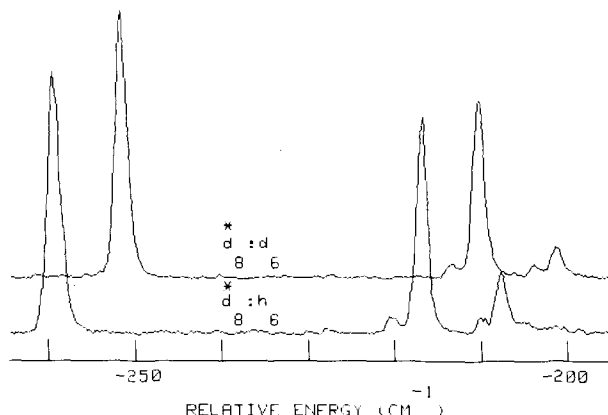


FIG. 5. Two-color mass spectra of  $d_8^*:d_6$  and  $d_8^*:h_6$  near the  $0_0^0$  of the parallel displaced configuration of  $d_8:h_6$ . Energy scale is relative to the  $d_8^* 0_0^0$  at 37 671.5  $\text{cm}^{-1}$ . Note the unusual isotopic shifts (see Table IV). Experimental conditions (see Fig. 2).

TABLE IV. The  $0_0^0$  and  $6b_0^1$  bands of isotopically substituted toluene-benzene dimers.<sup>a</sup> All values are in  $\text{cm}^{-1}$ .

Transitions	$h_8^*$ vac. $\nu$	$h_8^*:d_6$ $\Delta\nu_d^h$	$h_8^*:h_6$ $\Delta\nu_h^h$	$\Delta\nu_d^h - \Delta\nu_h^h$	$d_6^*$ vac. $\nu$	$d_6^*:d_6$ $\Delta\nu_d^d$	$d_6^*:h_6$ $\Delta\nu_h^d$	$\Delta\nu_d^d - \Delta\nu_h^d$
$0_0^0$	37 477.5	-242.7	-247.0	4.3	37 671.5	-251.9	-259.8	7.9
$6b_0^1$	38 007.5	-243.1	-246.0	2.9	38 178.5	-249.9	-255.1	5.2

<sup>a</sup> $\Delta\nu_d^h$ —energy difference between  $h_8^*:d_6$  and  $h_8^*$ ,  $\Delta\nu_h^h$ —energy difference between  $h_8^*:h_6$  and  $h_8^*$ ,  $\Delta\nu_d^d$ —energy difference between  $d_6^*:d_6$  and  $d_6^*$ ,  $\Delta\nu_h^d$ —energy difference between  $d_6^*:h_6$  and  $d_6^*$ .

## B. Benzene dimer

Although the benzene dimer has been examined in the jet through two-color MS,<sup>8,9</sup> fluorescence,<sup>4</sup> and MBER experiments,<sup>6,7</sup> results for the toluene-benzene dimer suggest that the previous determination of the benzene dimer conformation and excited state dynamics might well require revision. The Discussion section will deal with the interpretation of these data in terms of excitation exchange theory.

### 1. Two-color MS

The absorption spectrum of the benzene dimer exhibits only one band, red shifted by  $\sim 40 \text{ cm}^{-1}$  relative to the benzene monomer electronic origin. A doublet is observed for the  $6_0^1$  transition together with three weak features (see Figs. 6 and 7), previously assigned as van der Waals modes of the benzene dimer.<sup>8</sup> The data are summarized in Table V.

### 2. Lifetimes

$S_1$  lifetimes have been obtained for  $h_8^*:h_6$ ,  $h_8^*:d_6$ ,  $d_6^*:d_6$ , and  $d_6^*:h_6$  at the  $0_0^0$  levels. Results are tabulated in Table III. Note the short lifetime of the benzene dimer as compared to that of the monomer.

### 3. Isotope effects

A study of the isotope effects for the benzene dimer has been reported for the  $6_0^1$  transition.<sup>9</sup> However, without information on the  $0_0^0$  transition, interpretation of these data are incomplete. Thus, we have carried out a systematic study of the isotope effect for the benzene dimer for both the  $0_0^0$  and  $6_0^1$  transitions (see Figs. 6 and 7 and Table V). No significant differences are found for the  $6_0^1$  transition between the previously reported isotope effects and those reported in this work. Note in particular that for both the  $0_0^0$  and  $6_0^1$  transi-

tions the homomolecular dimers ( $h_8^*:h_6$  and  $d_6^*:d_6$ ) always appear to lower energy than the mixed dimers ( $h_8^*:d_6$  and  $d_6^*:h_6$ ). This is clearly not associated with a normal isotope effect.

### 4. Miscellaneous experiments

Two other experiments have been carried out for the benzene dimer: a Stark effect investigation and a two photon absorption study of the  $0_0^0$  transition. Both experiments are designed to locate any hidden or forbidden transitions. Both experiments produce negative results.

The voltage at the TOFMS ionization region was varied from 300 to 2000 V/cm. No broadening of the  $h_8^*:h_6$   $0_0^0$  transition is observed over this range of Stark voltages.

A search for the two photon absorption of the  $0_0^0$  transition was not successful. A two photon spectrum would arise in this region if a  $g$ -symmetry exciton state were present. In order to test out this method, however, we search for a two photon absorption of  $n$ -propyl-benzene at the  $0_0^0$  transition. This experiment was also unsuccessful indicating that the two photon signal is about  $10^5$  times smaller than the one photon signal. If the ionization beam is focused, a small signal due to nonresonant four-photon ionization can be observed.

## C. Toluene dimer

### 1. Two color MS

Absorption spectra of the toluene dimer are presented for the  $0_0^0$  region only. Spectra of the higher vibronic transitions are omitted due to spectral congestion. Figure 8 (bottom trace) shows the absorption spectrum of  $h_8^*:h_8$  near the toluene monomer electronic origin. The absorption spectrum consists of sharp and diffuse features with an underly-

TABLE V. The  $0_0^0$  and  $6_0^1$  bands of isotopically substituted benzene dimers.<sup>a</sup> All values are in  $\text{cm}^{-1}$ .

Transitions	$h_8^*$ (vac. $\nu$ )	$h_8^*:d_6$ $\Delta\nu_d^h$	$h_8^*:h_6$ $\Delta\nu_h^h$	$\Delta\nu_d^h - \Delta\nu_h^h$	$d_6^*$ (vac. $\nu$ )	$d_6^*:h_6$ $\Delta\nu_h^d$	$d_6^*:d_6$ $\Delta\nu_d^d$	$\Delta\nu_h^d - \Delta\nu_d^d$
$0_0^0$	38 086.1 <sup>b</sup>	-38.7	-42.0	3.3	38 289.1 <sup>b</sup>	-39	-42.2	3.2
$6_0^1$	38 608.7	-41.8	-43.1	1.3	38 787.3	-41.5 <sup>c</sup>	-44.2 <sup>c</sup>	2.7
		-38.0	-39.4	1.4				

<sup>a</sup> $\Delta\nu_d^h$ —energy difference between  $h_8^*:d_6$  and  $h_8^*$ ,  $\Delta\nu_h^h$ —energy difference between  $h_8^*:h_6$  and  $h_8^*$ ,  $\Delta\nu_h^d$ —energy difference between  $d_6^*:h_6$  and  $d_6^*$ ,  $\Delta\nu_d^d$ —energy difference between  $d_6^*:d_6$  and  $d_6^*$ .

<sup>b</sup> See Ref. 19.

<sup>c</sup> Measured from the band maximum (see Fig. 7).

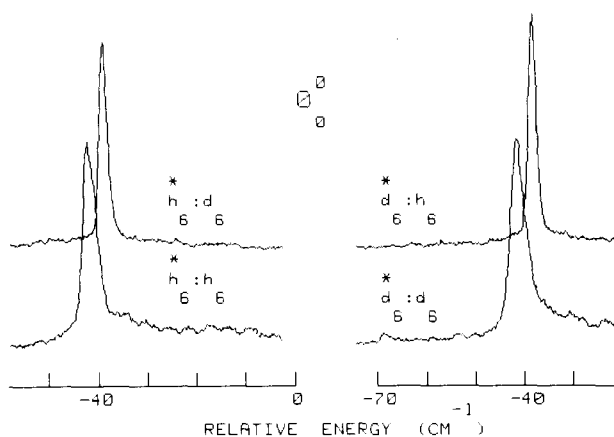


FIG. 6. Two-color mass spectra of  $h_6^*:d_6$ ,  $h_6^*:h_6$ ,  $d_6^*:h_6$ , and  $d_6^*:d_6$  at the  $0_0^0$ . Note that the homomolecular dimers are always to lower energy of the heteromolecular dimers (see Table V). Energy scales are relative to the  $0_0^0$  of  $h_6^*$  ( $38\,086.1\text{ cm}^{-1}$ ) and  $d_6^*$  ( $38\,289.1\text{ cm}^{-1}$ ). Experimental conditions: (see Fig. 2).

ing broad background. Similar spectra obtained for  $h_8^*:d_8$ ,  $d_8^*:d_8$ , and  $d_8^*:h_8$  (see Figs. 8 and 9).

The absorption features of  $h_8^*:d_8$  seem to be somewhat sharper than those of the other isotopes. Although large toluene clusters, (toluene)<sub>3</sub>, (toluene)<sub>4</sub>, etc. have absorption in the same region, fragmentation has been found to be minimal. Moreover, the absorption intensity of (toluene)<sub>3</sub> and (toluene)<sub>4</sub> for the beam conditions employed is found to be at least a factor of 10 smaller than that found for (toluene)<sub>2</sub>. The relative positions of the major absorption bands for (toluene)<sub>2</sub> are listed in Table VI.

## 2. Lifetimes

The  $S_1$  lifetime data for the major absorption features of (toluene)<sub>2</sub> with toluene expanded in a 0.5 mm pulsed nozzle are listed in Table VI. The nozzle temperature is maintained at 4 °C during this experiment. Relatively shorter lifetimes (by ~10 ns) are obtained for most of the absorption features (see Table VI) of  $h_8^*:h_8$  with a 25  $\mu\text{m}$  cw nozzle at 25 °C or a

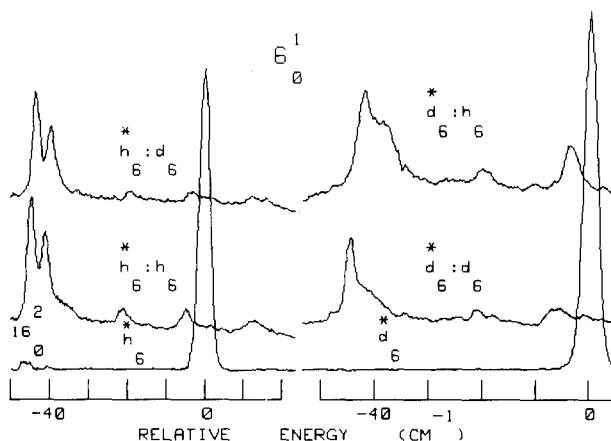


FIG. 7. Two-color mass spectra of  $h_6^*:d_6$ ,  $h_6^*:h_6$ ,  $d_6^*:h_6$ , and  $d_6^*:d_6$  at the  $6_0^1$ . In all cases, the homomolecular dimer are found to lower energy of the heteromolecular dimers (see Table V). Energy scales are relative to the  $6_0^1$  of  $h_6^*$  ( $38\,608.7\text{ cm}^{-1}$ ) and  $d_6^*$  ( $38\,787.3\text{ cm}^{-1}$ ). Experimental conditions (see Fig. 2).

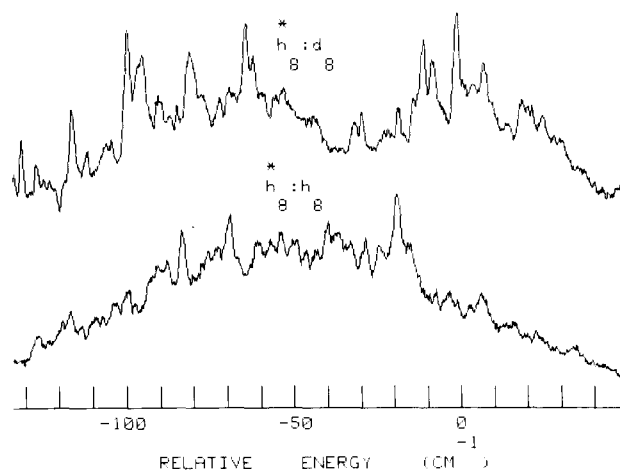


FIG. 8. Two-color mass spectra of  $h_8^*:d_8$  and  $h_8^*:h_8$  near the toluene electronic origin. Energy scale is relative to the  $h_8^* 0_0^0$ . Experimental conditions: 0.5 mm pulsed nozzle, backing pressure = 100 psi, nozzle temperature = 4 °C,  $\lambda_I = 3029\text{ \AA}$ .

0.5 mm pulsed nozzle at 70 °C. The  $S_1$  lifetime appears to be sensitive to beam conditions and cooling. Note also that relatively shorter lifetimes are found for  $d_8^*:h_8$  and that relatively longer lifetimes are found for  $d_8^*:d_8$ . We do not fully understand this behavior at present. The detailed structure of the excited state energy hypersurface and precisely where on this surface the molecule resides seem to play an essential role in determination of the  $S_1$  lifetimes of the dimeric isotopic species of toluene.

## 3. Ionization energy dependence

All isotopic dimers of toluene show two different energy dependences for the ionization energy. The more red shifted (broad) features have a lower ionization energy than the less red shifted (sharp) features (see Figs. 10 and 11). This is the same trend that is observed for the toluene–benzene dimer.

## 4. Isotope effects

Isotope effects for the toluene dimer have been examined for the  $0_0^0$  transition. The spectra and data can be found

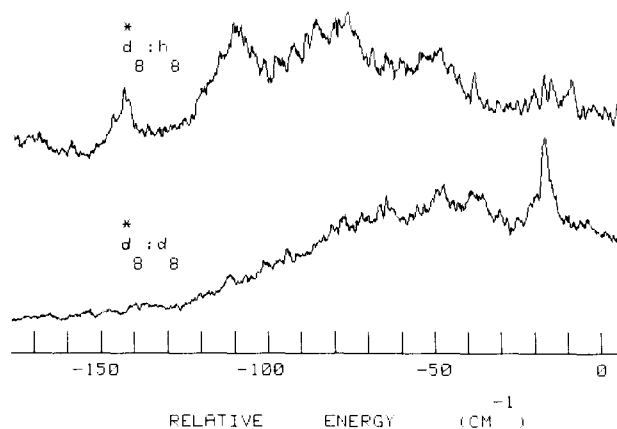


FIG. 9. Two-color mass spectra of  $d_8^*:h_8$  and  $d_8^*:d_8$  near the toluene  $-d_8$  electronic origin. Energy scale is relative to the  $d_8^* 0_0^0$ . Experimental conditions (see Fig. 8).

TABLE VI. The  $S_1$  lifetime  $\tau$  and spectral shifts (relative to the respective toluene  $0_0^0$ ) of the major bands of isotopically substituted toluene dimers near the toluene electronic origin (in ns and  $\text{cm}^{-1}$ ).

Bands shifts <sup>a</sup> ( $\text{cm}^{-1}$ )	$h_8^*:h_8$			$h_8^*:d_8$		$d_8^*:d_8$		$d_8^*:h_8$	
	$\tau$ , cw <sup>b</sup> (ns)	$\tau$ , $P_{\text{cold}}$ <sup>c</sup> (ns)	$\tau$ , $P_{\text{hot}}$ <sup>d</sup> (ns)	Band shifts ( $\text{cm}^{-1}$ )	$\tau$ , $P_{\text{cold}}$ <sup>c</sup> (ns)	Band shifts ( $\text{cm}^{-1}$ )	$\tau$ , $P_{\text{cold}}$ <sup>c</sup> (ns)	Band shifts ( $\text{cm}^{-1}$ )	$\tau$ , $P_{\text{cold}}$ <sup>c</sup> (ns)
-91	45			-101	65	-49		-143	38
-84	50	60	48	-81	60	-38	76	-111	39
-70	47	57	47	-65	61	-18	71	-87	40
-57	52			-54				-77	
-37	48	60	49	-32				-52	44
-20	75	72		-15	75			-17	
-4				-3	70			-10	46
5				6					

<sup>a</sup>Shifts of  $h_8^*:h_8$  and  $h_8^*:d_8$ , and  $d_8^*:d_8$  and  $d_8^*:h_8$ , are relative to the  $h_8^*$  and  $d_8^*0_0^0$ , respectively. Observable intensities of  $h_8^*:h_8$  and  $h_8^*:d_8$  extends to  $-250 \text{ cm}^{-1}$  relative to the  $h_8^*0_0^0$ .

<sup>b</sup>Lifetimes  $\tau$  employing a  $50 \mu\text{m}$  cw nozzle, nozzle temp =  $25^\circ\text{C}$ , backing pressure = 200 psi.

<sup>c</sup>Lifetimes  $\tau$  employing a 0.5 mm plused nozzle, nozzle time =  $4^\circ\text{C}$ , backing pressure = 100 psi.

<sup>d</sup>Lifetimes  $\tau$  employing a 0.5 mm plused nozzle, nozzle time =  $70^\circ\text{C}$ , backing pressure = 25 psi.

in Figs. 8 and 9 and Table VI. However, due to the complicated, broad structure of the spectrum, the isotopic effects cannot readily be assigned or compared.

#### IV. DISCUSSION

The intermolecular interactions and energy dynamics of the dimers can now be addressed based on the results presented in the last section. We will discuss the three systems separately. Since the toluene-benzene dimer has been pivotal in our understanding of the other dimers, we will discuss it first.

##### A. Toluene-benzene dimers

###### 1. Geometry

The absorption spectrum of  $h_8^*:h_8$  clearly shows two sets of absorption bands. These features have been associated with two distinct configurations. The absorption features of the lower energy set can be analyzed as a  $0_0^0$  transition fol-

lowed by a progression in a van der Waals stretch. The absorption features of the higher energy set are not readily analyzed in this fashion (see Figs. 1 and 2 and Table I). These two sets of features are apparently unrelated; i.e., the higher energy set is not built on the lower energy one. The features also have different ionization energies. The higher energy set of transitions near the toluene  $0_0^0$  has an ionization energy at least  $600 \text{ cm}^{-1}$  higher than the lower energy set. Other differences have been noted in the Results section.

As all the absorption features associated with the higher energy grouping have the same ionization energy dependence and similar spectral shifts, they must arise from similar conformations. This pattern would seem to be most likely generated by a perpendicular arrangement of the toluene and benzene molecules. Several possible orientations of the toluene and benzene molecules can give rise to a perpendicular arrangement; this would in turn generate a number of different transitions with similar energies.

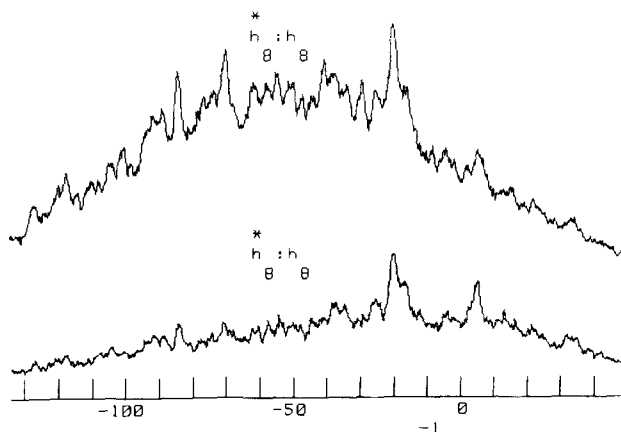


FIG. 10. Top trace: two-color mass spectrum of  $h_8^*:h_8$ . Bottom trace: one-color TOF mass spectrum of  $h_8^*:h_8$ . Energy scale is relative to the  $h_8^*0_0^0$ . Note the different ionization dependence of the absorption features. Experimental conditions (see Fig. 8).

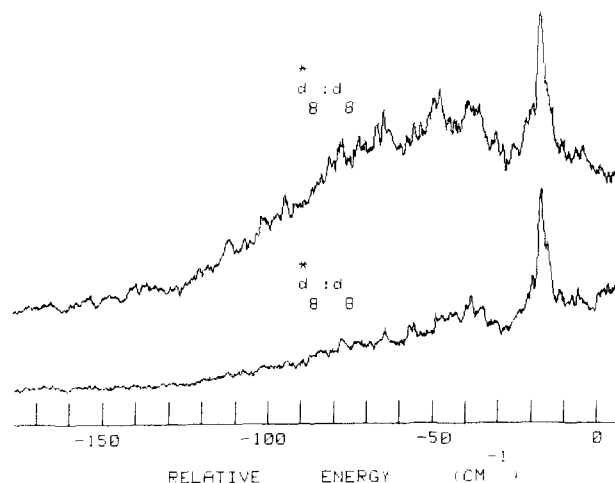


FIG. 11. Top trace: two-color mass spectrum of  $d_8^*:d_8$ . Bottom trace: one-color TOF mass spectrum of  $d_8^*:d_8$ . Energy scale is relative to the  $d_8^*0_0^0$ . Again, note the different ionization energy dependence of the absorption features. Experimental conditions (see Fig. 8).

The more red shifted bands appear to arise from a single conformation of  $h_8^*:h_6$ . Based on intensities, this conformation is favored by roughly 10:1 over the perpendicular ones. We assign these features to a parallel displaced configuration for the following reasons: (i) comparison with benzene discussed below; (ii) the parallel displaced conformation can easily transform into an excimer upon excitation; and (iii) given that the higher energy features are thought to arise from a perpendicular geometry, the parallel displaced geometry seems most reasonable.

Two parallel displaced geometries are possible. Polarizability arguments would favor the methyl group of toluene coordinated with center of the benzene ring. Hydrogen repulsion considerations would favor the methyl group away from the benzene ring. At present we are not able to resolve these geometries further, but it seems clear from the data that only one arrangement exists. Preliminary atom-atom potential calculations (exp-6) seem to favor the benzene displaced toward the methyl group.<sup>17</sup>

We should expect to observe a similar spectral pattern for  $h_8^*:h_8$ . The two-color MS spectrum of  $h_8^*:h_8$  (see Fig. 3 and Table II) at  $6_0^1$  consists of an intense doublet red shifted by  $45\text{ cm}^{-1}$  and a few weak, less red shifted features. We suggest that the  $-45\text{ cm}^{-1}$  band is the  $6_0^1$  transition of the parallel displaced conformation. The less red shifted features may partly be due to the perpendicular conformations of  $h_6:h_8$  and partly due to the van der Waals modes of the parallel displaced configuration. The intensity distribution is consistent with that observed for  $h_8^*:h_6$ .

The doublet nature of the  $6_0^1$  of  $h_8^*:h_8$  is caused by the lifting of the degeneracy of the  $h_6$   $6^1$  state due to the reduced site symmetry in the dimer (site splitting). The site splitting for  $6^1 h_8^*:h_8$  is about  $4.5\text{ cm}^{-1}$  and is similar to that observed in  $h_8^*:h_6$  (see below) and the benzene crystal.<sup>18</sup>

While the geometry designations for the different sets of transitions are based on comparisons, reasonability arguments, qualitative data, and preliminary calculations, the conclusion that two distinct general geometric arrangements exist for the toluene-benzene dimer is certain. This point is one that deserves emphasis and the one that has given us the insight into the structure of the benzene and toluene dimers discussed below. The parallel displaced and perpendicular arrangements are the best suggestions at this time for the two geometries.

## 2. Isotope effects

The mixed dimer  $h_8^*:h_6$  transitions are red shifted relative to the  $h_8^*$  monomer transitions, in general. This shift is due to additional stabilization of the excited state upon complexation. Thus, one expects that the  $h_8^*:d_6$  transition will be lower in energy than the  $h_8^*:h_6$  transition. As can be seen in Figs. 2, 4, and 5 and Table IV, this is the opposite of what is actually observed. As the  $S_1$  states of toluene and benzene are separated by more than  $600\text{ cm}^{-1}$ , spectral shifts due to quasiresonance interactions between the constituent molecules should be negligible. Studies of isotopic mixed crystals of benzene show that isotopic effects on the gas to crystal shifts ( $\Delta D$ ) are different for  $h_6$  in  $d_6$  ( $15\text{ cm}^{-1}$ ) and  $d_6$  in  $h_6$

( $-9\text{ cm}^{-1}$ ).<sup>19</sup> The mixed dimer in the gas phase could be subjected to similar effects. The energy difference between  $h_8^*:h_6$  and  $h_8^*:d_6$  and  $d_8^*:d_6$  and  $d_8^*:h_6$  can then be analyzed as a combination of the normal isotopic effect and the isotope effect on the gas to cluster shift. This analysis yields large normal isotopic effects—  $-12\text{ cm}^{-1}$  for the  $0_0^0$  and  $-8.6\text{ cm}^{-1}$  for the  $6b_0^1$  transitions. Unfortunately, no mixed crystal data are available for this system and direct comparison cannot be made. These values appear large to us and may well be hiding additional interactions not considered in the above analysis.

## 3. Excited state dynamics

Benzene and toluene molecules are known to form excimers in solution.<sup>20</sup> Toluene does not form an excimer as readily as benzene, supposedly due to steric hindrance between the methyl groups.<sup>20</sup> The present  $S_1$  lifetime data for  $h_8^*:h_6$  show a gradual shortening from the  $0^0$  to  $12^1$  states and eventually approach the 36 ns lifetime for  $6^1$  of  $h_8^*:h_8$ . This shortening of the  $S_1$  lifetime can be attributed to three apparent causes: (i) intramolecular vibrational redistribution (IVR); (ii) intersystem crossing; and (iii) excimer formation with a finite energy barrier. Since the  $S_1$  lifetime data are obtained by monitoring the intensity of the  $(h_8:h_6)^+$  ions, IVR has no impact on the observed lifetime as long as the employed ionization energy will ionize the  $h_8^*:h_6$   $0^0$ . Intersystem crossing seems unlikely to affect the toluene benzene lifetime because the  $S_1$  lifetimes of higher benzene clusters are not shortened.<sup>8</sup> We therefore suggest that the shortening of the  $S_1$  lifetime of the toluene-benzene dimer is an indication of excimer formation. The parallel displaced configuration changes to a parallel undisplaced and more tightly bound configuration. The observations that the lifetime of the  $0^0$  level is long and that the lifetimes of the  $12^1$  level of  $h_8^*:h_6$  and the  $6^1$  level of  $h_8^*:h_8$  are short give some idea of the barrier height for excimer formation. As  $12^1$  is  $933\text{ cm}^{-1}$  higher in energy than the  $0^0$ , we suggest that the barrier height is  $\sim 900\text{ cm}^{-1}$ .

## B. Benzene dimer

### 1. Geometry

To obtain a clear picture of the relative orientation of the benzene molecules in the benzene dimer, a discussion of the intermolecular interactions is necessary.

For the  $0_0^0$  transition or any totally symmetric vibration built on it, the benzene dimer energy can be written as<sup>21</sup>

$$E = \epsilon + D \pm M_{12}$$

in which  $\epsilon$  is the molecular transition energy,  $D$  is the gas to cluster shift and  $M_{12}$  is the exciton or excitation exchange energy. If the two components in the dimer are not symmetry related (i.e., not equivalent), then the gas to cluster shift terms can be different for each molecule and the above equation becomes slightly more complicated.

The observed spectrum will be strongly dependent on the symmetry of the dimer. If the two monomer units are in a parallel undisplaced configuration (i.e., the threefold axis is preserved in the dimer), no absorption will be observed for

the  $0_0^0$  transition and no site splitting will be observed for  $6_0^1$ . With lower than  $C_3$  symmetry either one or two dimer features can appear at the  $0_0^0$  transition and the  $6_0^1$  transition will split.

The details of the spectra also depend on the intermolecular interactions. Since only one absorption feature appears at the  $0_0^0$  for each dimer and the  $6_0^1$  is a doublet, certain severe restriction are placed on the geometry of  $(\text{benzene})_2$ .

As can be seen from the spectra of the  $0_0^0$  region, the isotope effects are relatively small and do not dominate the line positions (Fig. 6). However, exciton effects do control the separation between the isotopic dimers ( $h_6^*:h_6$  and  $h_6^*:d_6$ ;  $d_6^*:d_6$  and  $d_6^*:h_6$ ), as the homomolecular or "pure" dimers are *always lower in energy* than the heteromolecular or "mixed" dimers. The energy separation  $\Gamma$  between  $h_6^*:h_6$  and  $h_6^*:d_6$  and  $d_6^*:d_6$  and  $d_6^*:h_6$  can be analyzed as follows:

$$\Gamma = \Delta + \Delta D + \delta + M_{12}$$

in which  $\Delta$  is the isotope effect,  $\Delta D$  is the isotope effect on the gas to cluster shift, and  $\delta$  is the quasiresonance term.<sup>21</sup> The contribution of the terms  $\Delta$ ,  $\Delta D$ , and  $\delta$  to  $\Gamma$  have different signs for the  $h_6^*$  dimers and  $d_6^*$  dimers; the  $M_{12}$  term, however, always has the same sign. One then finds

$$(3.32 \text{ cm}^{-1})_{h_6^*} = -\Delta + \Delta D - \delta + M_{12},$$

$$(3.17 \text{ cm}^{-1})_{d_6^*} = \Delta - \Delta D' + \delta + M_{12},$$

or

$$6.49 \text{ cm}^{-1} = \Delta D - \Delta D' + 2M_{12}.$$

From the study of isotopic mixed benzene crystals,<sup>19</sup> one finds that  $\Delta D' = 3/5 \Delta D$ . Thus for the  $0_0^0$  transition,

$$2M_{12} + 2/5 \Delta D = 6.49 \text{ cm}^{-1}.$$

Given the above observations, the benzene dimer must be such that the two molecules are symmetry related (equivalent). The transition to the upper exciton component is spectroscopically forbidden. Two such arrangements of the monomer subunits can give rise to the observations: (i)  $D_{2h}$  symmetry with bond subunits lying in the same plane; and (ii)  $C_{2h}$  symmetry with the molecules parallel, stacked, and displaced. The first configuration seems unlikely based on hydrogen repulsion and excimer formation. The  $C_{2h}$  parallel displaced conformation is favored. The most reasonable displaced geometry probably minimizes the repulsion energy. We believe this would imply a displacement along the  $y$  axis (through a carbon atom). The allowed transitions in  $C_{2h}$  symmetry is  $A_u \leftarrow A_g$  and the forbidden transition is  $B_g \leftarrow A_g$ . In this geometry, the dimer does not have a ground state dipole moment.

Similar spectra are observed for the nontotally symmetric vibronic transition  $6_0^1$ . Note the peculiar line shapes for the  $6_0^1$  transition of  $d_6^*:h_6$  and  $d_6^*:d_6$ . This may be due partly to the increase in the line width of the excitation laser to  $\sim 1 \text{ cm}^{-1}$ , a result of mixing  $1.06 \mu\text{m}$  with doubled LDS 698. Employing reasoning comparable to that for the  $0_0^0$  transition to analyze the  $6_0^1$  features, we find

$$2M'_{12} + 2/5 \Delta D = 3.99 \text{ cm}^{-1}$$

in which  $M'_{12}$  is virtually zero based on a comparison of pure and isotopically mixed benzene crystal data<sup>22</sup> and similar values of the site splitting in  $h_6^*:h_6$  and  $h_6^*:d_6$ . Thus,  $\Delta D$  is approximately equal to  $10 \text{ cm}^{-1}$ . If we set  $\Delta D(6_0^1) = \Delta D(0_0^0)$ , then  $M_{12} \sim 1.3 \text{ cm}^{-1}$ . This value is similar to the various values found for the benzene crystal, albeit with the benzene molecules in a different orientation.<sup>21</sup> The  $6^1$  site splitting obtained in the present study is  $\sim 3.6 \text{ cm}^{-1}$  which is nearly identical to that found for the benzene crystal.<sup>18</sup> All these results are consistent with a  $C_{2h}$  dimer symmetry.

The value of  $M_{12}$  for the  $0^0$  of  $(\text{benzene})_2$  can also be determined based on the observed energies for the  $0_0^0$  and  $6_0^1$  transitions of  $h_6^*:h_6$  and  $h_6^*:d_6$ .<sup>21</sup> The vibrational intervals of a guest in an isotopic mixed benzene crystal are independent of isotopic substitution of the host. Thus, the value found for  $6^1$  in  $h_6^*:d_6$  ( $521.4 \text{ cm}^{-1}$ ) should be the true value of  $6^1$  in the dimer. In addition, the nontotally symmetric vibrations in a pure isotopic crystal or dimer carry little or no exciton splitting and are built on the exciton *band center*, not one of the exciton levels.<sup>23</sup> The measured  $6^1-0^0$  separation for  $h_6^*:h_6$  is  $523.3 \text{ cm}^{-1}$ , but, based on this reasoning, the true  $6^1-0^0$  separation is  $521.4 \text{ cm}^{-1}$ . The exciton band center is thus  $1.9 \text{ cm}^{-1}$  higher than the observed  $h_6^*:h_6$  lower energy exciton band component. This method of calculating the exciton interaction yields  $M_{12} \sim 1.9 \text{ cm}^{-1}$ . Similar estimates can be made for  $d_6^*:d_6$ ,  $d_6^*:h_6$  dimers, but the  $6_0^1$  transitions in these dimers are not well resolved. An accurate value of  $6^1$  for  $d_6^*$  is thus not readily available.

The analysis of the  $0_0^0$  exciton band based on just the  $0_0^0$  transitions of  $h_6^*:h_6$ ,  $h_6^*:d_6$  and  $d_6^*:d_6$ ,  $d_6^*:h_6$  gives the band center  $\sim 1.3 \text{ cm}^{-1}$  above the observed homodimer origins and a value of  $M_{12}$  equal to  $\sim 1.3 \text{ cm}^{-1}$ . Considering the various assumptions made in both calculations, the best value of  $M_{12}$  is probably an average of these estimates, therefore,  $M_{12} \sim 1.6 \text{ cm}^{-1}$ .

The benzene dimer was previously suggested to be polar based on a MBER study.<sup>6,7</sup> This work concludes that the dimer has  $C_{2v}$  symmetry with the two benzene molecules perpendicularly arranged relative to one another. We believe that this perpendicular  $C_{2v}$  arrangement is a reasonable one based on these data and the benzene crystal data. As can be seen in the benzene-toluene system, two different conformations are possible even though the parallel displaced (low transition energy) conformation is dominant for our beam condition. If the statistical distribution between the two possible geometries for the benzene dimer is the same as for the toluene-benzene dimer, we would probably not be able to detect the perpendicular configuration of the benzene dimer.

A recent calculation<sup>12(g)</sup> suggests that the benzene dimer geometry is close to the parallel stacked displaced configuration but with the "ligand" ring tilted out of the plane by  $\sim 26^\circ$  (i.e.,  $\_ \setminus$ ). This calculation employs an exp-6-1 potential. The geometry calculated, however, is inconsistent with our spectroscopic data. Nonetheless, this potential gives a "local minimum" ( $-905$  vs  $-915 \text{ cm}^{-1}$ ) in the surface at the parallel stacked displaced  $C_{2h}$  configuration suggested by the present experimental data. We will discuss calculations for the benzene and toluene dimers in a subsequent publication.

## 2. Excited state dynamics

The shortening of the  $S_1$  lifetime of the benzene dimer with respect to the benzene monomer (36 vs 103 ns) has been attributed to excimer formation upon excitation.<sup>8</sup> The previous work suggests a transformation of a ground state perpendicular conformation to a parallel stacked (sandwich) excimer geometry. Based on the parallel displaced configuration determined in the last section, the excimer transformation must take the dimer from a parallel displaced configuration to a parallel stacked (undisplaced) configuration. The parallel displaced ground and nonexcimer excited state configuration of the benzene dimer would appear to facilitate the transformation, with zero energy barrier, to the excimer geometry.

## C. Toluene dimer

Due to the complexity of the toluene dimer spectrum, the geometry and excited state dynamics of this system cannot be elucidated with any certainty at present. However, the fact that the absorption bands exhibit different ionization energy dependence suggests that the toluene dimer has two different accessible configurations.

In the toluene benzene system, the more red shifted parallel displaced conformation has a lower ionization energy than the less red shifted perpendicular conformation. This same behavior is observed for the toluene dimer. The sharp features near  $-20 \text{ cm}^{-1}$  from the toluene monomer would then be associated with the perpendicular dimer and the broader features to the low energy side of the transition would be associated with the parallel displaced dimer (Figs. 8–11). The lifetime data for  $h^*_6:h_8$  seem to favor this general interpretation. However, the  $S_1$  lifetimes appear to be a function of beam conditions and isotopic substitution (Table VI); a firm conclusion therefore is difficult to reach.

The potential surfaces for these two species must be very close together at this energy and the spectra are clearly quite dependent on temperature and the exact positions of the energy levels. At the present time we can only be certain that at least two configurations for the toluene dimer exist and one of them has a reduced lifetime.

## V. CONCLUSION

Through the observation of lifetimes, absorption (two-color TOFMS detected), isotopic substitution, and ionization energy dependences, information has been gathered on three aromatic dimers—(benzene)<sub>2</sub>, (toluene–benzene), and (toluene)<sub>2</sub>. The ability to compare and contrast the behavior found for the three systems has also been of considerable assistance in determining their structure and dynamics. The important information obtained in this study can be summarized as follows:

(i) Two different conformations were observed for toluene–benzene and (toluene)<sub>2</sub>; in one conformation the molecules are arranged in a perpendicular fashion and in the other they are parallel and displaced. Only the parallel displaced configuration is observed for (benzene)<sub>2</sub> in these optical experiments. Both dimer geometries of the toluene and toluene–benzene systems, parallel and perpendicular, have a

similar enough binding energies to be present in the beam expansion simultaneously.

(ii) The cluster shifts for the  $S_1$  transitions of the parallel displaced configuration dimers are  $-40 \text{ cm}^{-1}$  for  $h^*_6:h_6$ ,  $-45 \text{ cm}^{-1}$  for  $h^*_6:h_8$ , and  $-250 \text{ cm}^{-1}$  for  $h^*_8:h_6$ . In the perpendicular configuration this shift is  $-25 \text{ cm}^{-1}$  for  $h^*_6:h_6$  and  $-20 \text{ cm}^{-1}$  for  $h^*_8:h_8$ . These shifts imply that the excited states are more tightly bound than the ground states.

(iii) The exchange or exciton splitting in the  $0^0$  level of (benzene)<sub>2</sub> has been found in two ways: an isotopic-exciton analysis of the  $0^0_0$  transition and a band center determination based on  $6^1$ . Each method has a number of assumptions and the values for  $M_{12}$  are  $1.3 \text{ cm}^{-1}$  and  $1.9 \text{ cm}^{-1}$ , respectively. The best estimate of  $M_{12}$  is probably  $\sim 1.6 \text{ cm}^{-1}$ .

(iv) The site splitting of  $6^1$  is  $3.6 \text{ cm}^{-1}$  in the benzene dimer.

(v) The parallel displaced conformation of the benzene and toluene–benzene dimers in the excited  $S_1$  state transform into an excimer geometry, thus shortening the excited state lifetimes. The barrier heights are  $\sim 0 \text{ cm}^{-1}$  for (benzene)<sub>2</sub> and  $\sim 900 \text{ cm}^{-1}$  for toluene–benzene.

Further work on these systems is being carried out in three different directions: (1) calculations of shifts and structures based on a number of different potentials; (ii) two-photon spectroscopy at much higher sensitivity; and (iii) asymmetric isotropic substitution studies.

*Note added in proof:* Further attempts to observe a two-photon allowed  $0^0_0$  transition of (benzene)<sub>2</sub> have also yielded negative results. The two-photon allowed  $14^1_0$  transition of C<sub>6</sub>H<sub>6</sub> is observed (TOFMS detected) to be strong ( $\sim 10 \text{ V}$  of signal). The (benzene)<sub>2</sub>  $14^1_0$  is also observed ( $\sim 400 \text{ mV}$ ). However, in the  $0^0_0$  region of (benzene)<sub>2</sub> no features are discernible above the  $20 \text{ mV}$  background signal indicating that the two-photon allowed (benzene)<sub>2</sub> origin is at least a factor of  $\sim 20$  less intense than the  $14^1_0$  of the dimer.

<sup>1</sup>(a) E. R. Bernstein, K. S. Law, and M. W. Schauer, *J. Chem. Phys.* **80**, 634 (1984); (b) A. Amirav, U. Even, and J. Jortner, *ibid.* **75**, 2489 (1981).

<sup>2</sup>C. A. Haynam, D. V. Brumbaugh, and D. H. Levy, *J. Chem. Phys.* **79**, 1581 (1983).

<sup>3</sup>D. E. Poeltl and J. K. McVey, *J. Chem. Phys.* **78**, 4349 (1983).

<sup>4</sup>P. R. R. Langridge-Smith, D. V. Brumbaugh, C. A. Haynam, and D. H. Levy, *J. Phys. Chem.* **85**, 3742 (1981).

<sup>5</sup>D. H. Levy, C. A. Haynam, and D. V. Brumbaugh, *Faraday Discussion No. 73, van der Waals Molecules*, St. Catherine's College, Oxford, (1982).

<sup>6</sup>K. C. Janda, J. C. Hemminger, J. S. Winn, S. E. Novick, S. J. Harris, and W. Klemperer, *J. Chem. Phys.* **63**, 1419 (1975).

<sup>7</sup>J. M. Steed, T. A. Dixon, and W. Klemperer, *J. Chem. Phys.* **70**, 4940 (1979).

<sup>8</sup>J. B. Hopkins, D. E. Powers, and R. E. Smalley, *J. Phys. Chem.* **85**, 3739 (1981).

<sup>9</sup>K. H. Kung, H. L. Selzle, and E. W. Schlag, *J. Phys. Chem.* **87**, 5113 (1983).

<sup>10</sup>G. E. Bacon, N. A. Curry, and S. A. Wilson, *Proc. R. Soc. London Ser. A* **279**, 98 (1964).

<sup>11</sup>N. Boden, P. P. Davis, C. H. Stam, and G. A. Wesselink, *Mol. Phys.* **25**, 81 (1973).

<sup>12</sup>(a) D. P. Craig, P. A. Dobish, R. Mason, and D. P. Santry, *Discuss. Faraday Soc.* **40**, 110 (1965); (b) K. Banerjee and L. Salem, *Mol. Phys.* **11**, 405 (1966); (c) A. I. M. Rae and R. Mason, *Proc. R. Soc. A* **304**, 487 (1968); (d) D. R. Williams and R. C. Shapiro, *J. Chem. Phys.* **54**, 4838 (1971); (e) D. Hall and D. E. Williams, *Acta Crystallogr. Sect. A* **31**, 56 (1975); (f) T. B.

- MacRury, W. A. Steele, and B. J. Berne, *J. Chem. Phys.* **64**, 1288 (1976); (g) D. E. Williams, *Acta Cryst. Allogr. Sect. A* **36**, 715 (1980).
- <sup>13</sup>E. R. Bernstein, K. Law, and Mark Schauer, *J. Chem. Phys.* **81**, 49 (1984).
- <sup>14</sup>K. Watanake, T. Nakayama, and J. Mottl, *J. Quant. Spectrosc. Radiat. Transfer* **2**, 369 (1962).
- <sup>15</sup>J. Jortner, U. Even, S. Leutwyler, and Z. Berkovitch-Yellin, *J. Chem. Phys.* **78**, 309 (1983).
- <sup>16</sup>S. M. Beck, M. G. Liverman, D. L. Monts, and R. E. Smalley, *J. Chem. Phys.* **70**, 232 (1979).
- <sup>17</sup>E. R. Bernstein and Mark Schauer (unpublished results).
- <sup>18</sup>(a) V. L. Broude, *Pure Appl. Chem.* **37**, 21 (1974); (b) E. R. Bernstein, *J. Chem. Phys.* **50**, 4842 (1969).
- <sup>19</sup>S. D. Colson and T. L. Netzel, *Chem. Phys. Lett.* **16**, 555 (1972).
- <sup>20</sup>J. B. Birks, *Rep. Prog. Phys.* **38**, 905 (1975).
- <sup>21</sup>S. D. Colson, *J. Chem. Phys.* **48**, 3324 (1968).
- <sup>22</sup>G. C. Nieman and G. W. Robinson, *J. Chem. Phys.* **39**, 1298 (1963).
- <sup>23</sup>E. R. Bernstein, S. D. Colson, R. Kopelman, and G. W. Robinson, *J. Chem. Phys.* **48**, 5596 (1968).